(Preprint) AAS 19-133

IN-FLIGHT LINE-OF-SIGHT POINTING PERFORMANCE FOR THE GOES-16 AND GOES-17 SPACECRAFT

Tim Bevacqua,[*] Jim Chapel,[†] Devin Stancliffe,[‡] Tim Rood,[§] Doug Freesland,[**] and Alexander Krimchansky[††]

The Geostationary Operational Environmental Satellite-R program (GOES-R) has launched two of the next generation geostationary weather satellites, both of which are now fully operational. GOES-16 launched in November 2016, and GOES-17 launched in March 2017. In this paper, we present the pointing and pointing stability results of the two spacecraft, with specific focus on aspects of the design related to mitigating jitter. The flight instrument suite includes 6 seismic accelerometers sampled at ~2 KHz, allowing in-flight verification of pointing stability and comparison back to simulation predictions. This paper compares the observed flight results with the simulation predictions for acceleration and shock response spectrum (SRS) for various operational scenarios and instrument observation modes. Passive isolation of both the reaction wheels and the payload deck have proved to be effective in reducing jitter responses. Active Vibration Damping (AVD) of flexible-body modes attenuates the low frequency motion of the vehicle appendages, improving the low-frequency pointing performance. Knowledge of the instrument scan mirror motion is fed forward to the reaction wheel control, reducing disturbances on the spacecraft bus. Attitude knowledge and rate data are provided to the primary Earth-observing instrument with an accuracy defined by the Integrated Rate Error (IRE) requirements. The data are used to adjust instrument scanning. As we show in this paper, the in-flight performance of the GN&C design provides the necessary capabilities to achieve the demanding GOES-R mission objectives while its robustness enabled the simultaneous operation of the Advanced Baseline Imager (ABI) prime and redundant cryocoolers (CCs) to resolve an in-flight cooling anomaly on GOES-17.

INTRODUCTION

GOES-16 and GOES-17 represent the first two spacecraft in the GOES-R series. They were launched in November 2016 and March 2017, respectively, and have proven highly successful in flight. The mission includes both Earth-observing and space weather instruments, hosting a communication payload to deliver instrument data to the data processing centers, serving as a data collection platform, and providing search and rescue services. In this paper we provide a look at flight data from GOES-16 and GOES-17, and we build upon design material previously presented.[1,2,3] Here we focus on the components of the design intended to mitigate Line-of-Sight (LOS) micro-vibrations due to on-board internal disturbances. Unique to this work are the GOES-17 in-flight results. Some are the same as GOES-16 (IRE and Predicted Interface Force and Torque (PIFT) feed-forward compensation), others are decidedly different (AVD parameters and the jitter disturbance environment with simultaneous CC operation).

[*] Lockheed Martin Space, Denver CO
[†] Ph.D., Lockheed Martin Space, Denver CO
[‡] Lockheed Martin Space, Denver CO
[§] Advanced Solutions Inc., Denver CO
[**] The ACS Engineering Corporation, Clarksville MD
[††] NASA GOES-R Flight Project, NASA Goddard Space Flight Center MD

Relative to the previous generation of GOES satellites, the GOES-R ABI, represents a quantum increase in Earth weather observation capabilities. ABI provides 4 times the resolution, 5 times the observation rate, 100 times data rate and 3 times the number of spectral bands for Earth observations.[4] In addition to ABI, a newly-developed Earth-observing instrument is hosted by the spacecraft—Geostationary Lightning Mapper (GLM). GLM is a near-infrared optical transient detector, which can detect extremely brief changes in an optical scene, indicating the presence of lightning. The configuration of these instruments on the GOES-R EPP is shown in Figure 1.

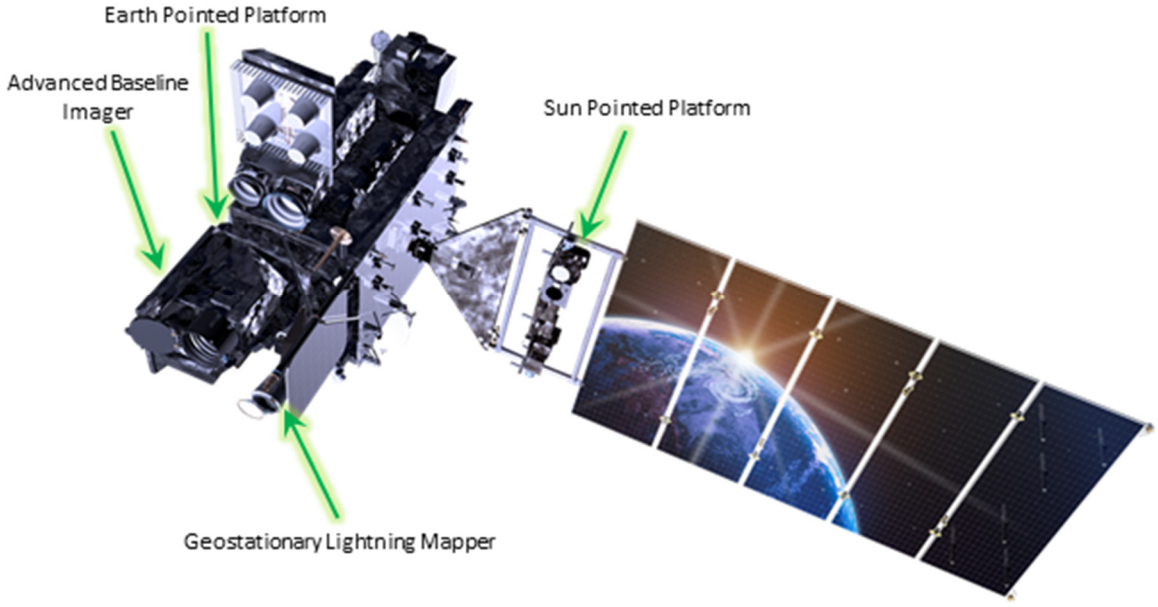

Figure 1. GOES-R Spacecraft in Operational Configuration.

While there were many aspects of the GOES-R design required to meet the stringent pointing and stability requirements, this paper will focus on the parts of the design intended to improve LOS performance. Following an overview of the GN&C design, the dual isolation concept is discussed, used to attenuate higher frequency jitter disturbances and includes ground and in-flight testing performed to validate the approach. This is followed by a discussion of the AVD and PIFT used to improve LOS performance at lower frequencies. PIFT is a spacecraft-to-instrument data interface used for LOS pointing improvement. The interface is two-way, with the ABI providing force and torque estimates from its two internal scan mirrors to the spacecraft controller for feed-forward compensation of induced transients, and the spacecraft providing 100 Hz angular rate to the ABI used for real-time LOS control to steer out jitter up to the first instrument mode.[5]

GOES-R GN&C DESIGN APPROACH

The stringent GOES-R attitude determination requirements dictate that the IMUs and star trackers be co-located with the Earth-observing instruments on the EPP. To meet the jitter requirements presented in the previous section, the EPP is designed as a stiff structure with the first structural mode at approximately 50 Hz. The EPP is constructed of carbon fiber facesheets over aluminum honeycomb, spans approximately 1.9 x 2.2 m, and has a thickness of about 0.15 m. The resulting configuration is shown in Figure 2, where the placement was driven by fields of regard for the instruments, and keep-out zones for the star trackers. The high stiffness of the optical bench readily transmits disturbances through the structure. To attenuate high frequency disturbances to the Earth-observing instruments, including reaction wheel disturbances, gimbal disturbances, and disturbances from the sun-pointed instruments, the EPP is passively isolated from the spacecraft bus with Honeywell D-Strut isolators[6] arranged in a modified Stewart-platform configuration.[7,8] The isolation system provides attenuation for frequencies above ~5 Hz in all six degrees-of-freedom.

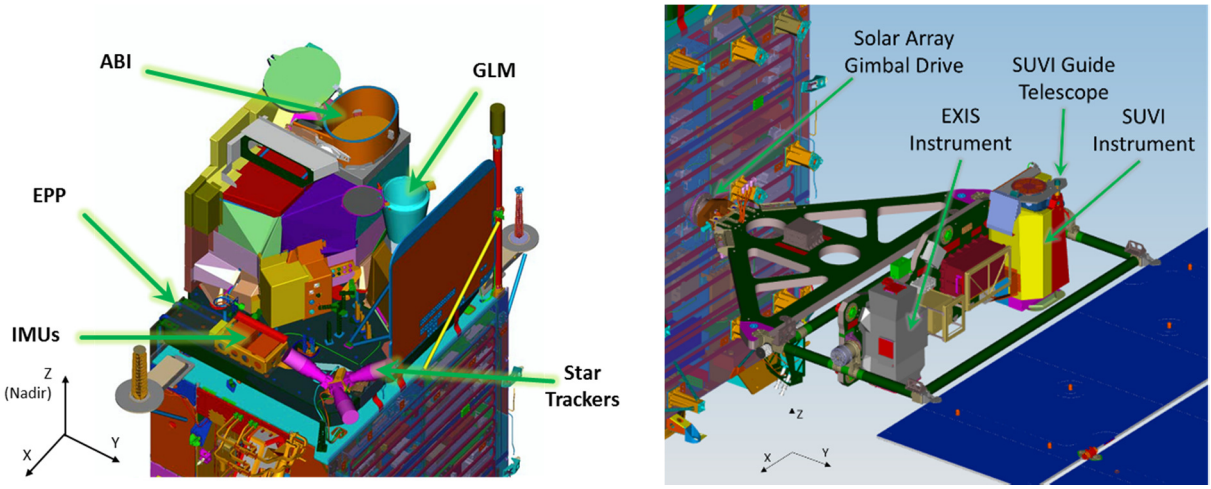

a) Earth Pointing Platform Configuration *b) Sun Pointed Platform (SPP) Configuration.*

Figure 2. GOES-R Earth and Sun Pointing Observatories.

The GOES-R spacecraft design utilizes 6 Honeywell HR-18 reaction wheels, arranged as shown in Figure 3. The wheels are mounted at the –Z end of the vehicle, far away from the EPP to reduce vibration to the instruments. The use of 6 wheels provides functional redundancy, reduced maximum speed (which decreases vibration), and relatively high torque capability. A secondary passive isolation system manufactured by Moog/CSA Engineering is implemented for each reaction wheel. The design is based upon Moog's Visco-Elastic Material (VEM) vibration isolation technology.[9] This secondary isolation system provides attenuation for frequencies above ~50 Hz for each wheel.

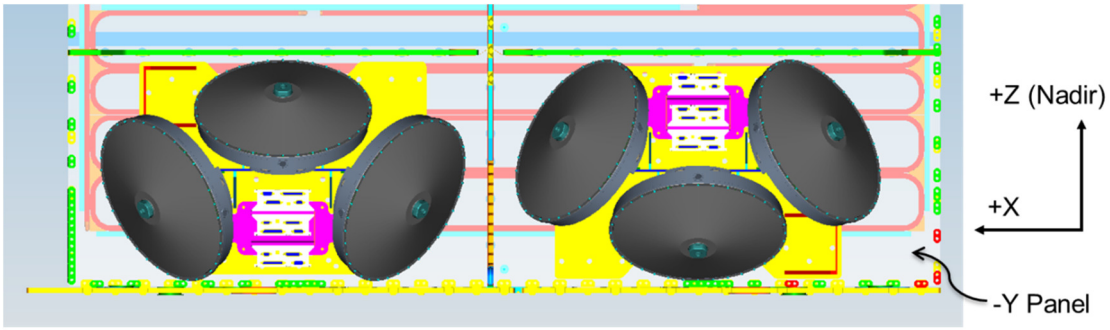

Figure 3. Reaction Wheel Configuration of the GOES-R Spacecraft.

Within the control design, there are a number of feedforward paths to facilitate the operate-through capability. Feedforward of the thruster torques during thruster operations is one feedforward path.[3] Additionally, ABI provides force and torque disturbance predictions for scan mirror motion. Freesland et al.,[10] demonstrated the effectiveness of using PIFT data to improve attitude stability performance by a factor of 5X. GOES-R includes feedforward compensation based on ABI's PIFT data.

To reduce the impact of low frequency disturbances, GOES-R has included AVD developed by Lockheed Martin.[11,12] This additional compensation phase stabilizes the first several structural modes, up to ~2 Hz. The first structural mode is at ~0.25 Hz, and is related to the large solar panel flexibility coupled with the deployment hinge stiffness. Although not truly a feed forward term, the AVD compensation is implemented within the architecture in a similar fashion. It has proven particularly effective for the first three structural modes on GOES-16 and GOES-17.

For attitude determination, GOES-R utilizes the Northrop Grumman Scalable Space Inertial Reference Unit (SSIRU) for the IMU, and the SODERN Hydra with three optical heads for the star tracker. The design includes 2 SSIRUs with 4 gyros each, but only one SSIRU is powered on at a time. The SSIRU was chosen for its high bandwidth and low latency rate output, and for its low-noise characteristics. The 4 gyros are sampled at 200 Hz, and the star tracker optical heads are sampled at 20 Hz. Attitude estimation is performed using a kinematic 6-state extended Kalman filter which combines quaternion outputs from the star tracker with angular rate measurements from the

SSIRU to produce a 3-state attitude error estimate and 3-state gyro bias error estimate.[13] As with previous GOES satellites, accurate attitude and rate estimates are critical to INR performance as they are used in the ground-based motion reconstruction and compensation. For GOES-R, rate estimates are also used for real-time ABI mirror control.[14,5] Two samples of 200 Hz gyro data are collected, filtered, bias-corrected and converted to 3-axis rate data before sending to ABI at 100 Hz.

Finally, the gimbal design used for the azimuth and elevation control of the solar array and SPP incorporates the proven low-disturbance design first implemented on the Mars Reconnaissance Orbiter.[15] The design is based upon a zero-backlash harmonic drive with a relatively high gear reduction of 200:1. A 2-phase brushless motor with sine-drive commutation provides a low disturbance capability, and effectively eliminates motor cogging. A high-bandwidth motor-rate control loop eliminates most of the harmonic drive friction and nonlinear effects. The high performance of the gimbals removes gimbal dynamics as a significant pointing and jitter disturbance source, while providing sub-arcsec pointing capability.[3]

DUAL ISOLATION AND JITTER PERFORMANCE

Jitter requirements for the nadir pointed instruments were cast in terms of linear translational accelerations and SRS at the instrument interfaces as shown in Figure 4. The requirements cover a broad frequency range out to 512 Hz. Two levels are shown, General Interface Requirements Document (GIRD) and Payload Resource Allocation Document (PRAD).[16.17] The instruments are designed to meet their performance requirements in the presences of the higher GIRD levels. The spacecraft is designed to produce disturbances no greater than the lower PRAD levels. The difference is government reserve.

Missions with stringent jitter requirements are often faced with the dilemma of isolating the payload sensitive to jitter, or isolating the source of the jitter itself. For the GOES-R series, this dilemma was solved electing a minimum risk, albeit not minimum cost, dual isolation approach. Requirements drove the EPP optical bench to be a stiff design, passively isolated from the spacecraft bus, providing attenuation in the lower frequency 5-30 Hz range. To reduce the risk of higher frequency RWA disturbances impacting jitter performance, a secondary passive isolation system was incorporated under each of the six RWAs tuned to provide attenuation at frequencies >50 Hz.

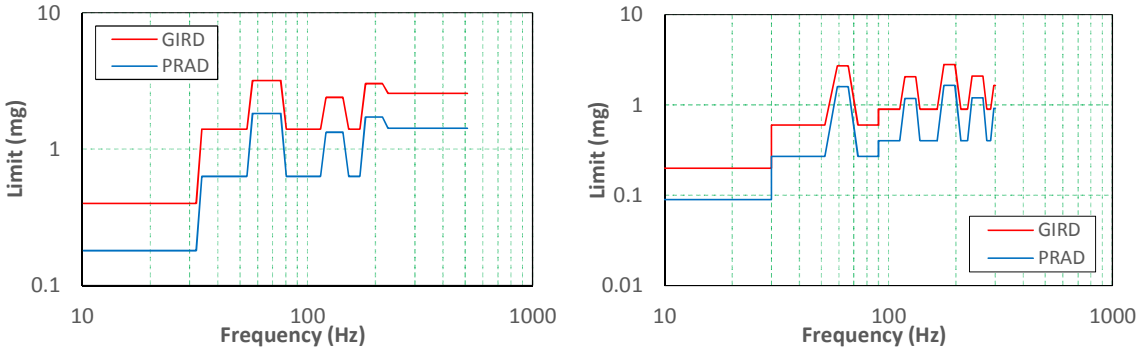

a) Linear translation acceleration limits.

b) Shock response spectra limits

Figure 4. Jitter Requirements were Cast in Terms of Acceleration and SRS at the Instrument Interface.

EPP and RWA Isolation Design and Bench Testing

To attenuate high frequency disturbances to the Earth-observing instruments from the spacecraft bus, including reaction wheel disturbances, gimbal disturbances, and disturbances from the sun-pointed instruments, the EPP is passively isolated from the spacecraft bus with flight-proven Honeywell D-Strut isolators arranged in a modified Stewart platform configuration.[6,7,8] The isolation system provides attenuation for frequencies above ~5 Hz in all six degrees-of-freedom. The mounting geometry and the strut parameters have been optimized to provide balanced isolation performance in all six degrees-of-freedom.

The GOES-R project undertook a full qualification effort for the EPP and isolation system. To demonstrate acceptable stability and isolation performance and to validate the simulation models, an EDU EPP with six D-Strut isolators arranged in a flight-like configuration was assembled and tested at Honeywell's facilities. The test configuration included mass simulators for the ABI and GLM instruments, as well as the GLM radiator. Mass

simulators were also included for the star trackers and IMUs. To assess the isolator performance impacts of parasitic shunts across the isolation interface, flight-like harnessing and multi-layer insulation blanketing were also included in the test configuration. Tests were run with and without the shunts present. The transmissibility results are shown in Figure 5 for the X and Y translation axes. As can be seen in the figure, the requirements are met for the EPP isolation with and without the shunts included. However, the shunts clearly affect the performance of the isolation system, and therefore cannot be neglected in the simulation models. The shunts are not symmetric with respect to the EPP layout, so some axes are affected more than others. Because of the impacts of the shunts on the overall dynamics, additional testing was performed to more accurately capture the shunts' effects. The results have been included in the high-fidelity simulation models of the EPP isolation.

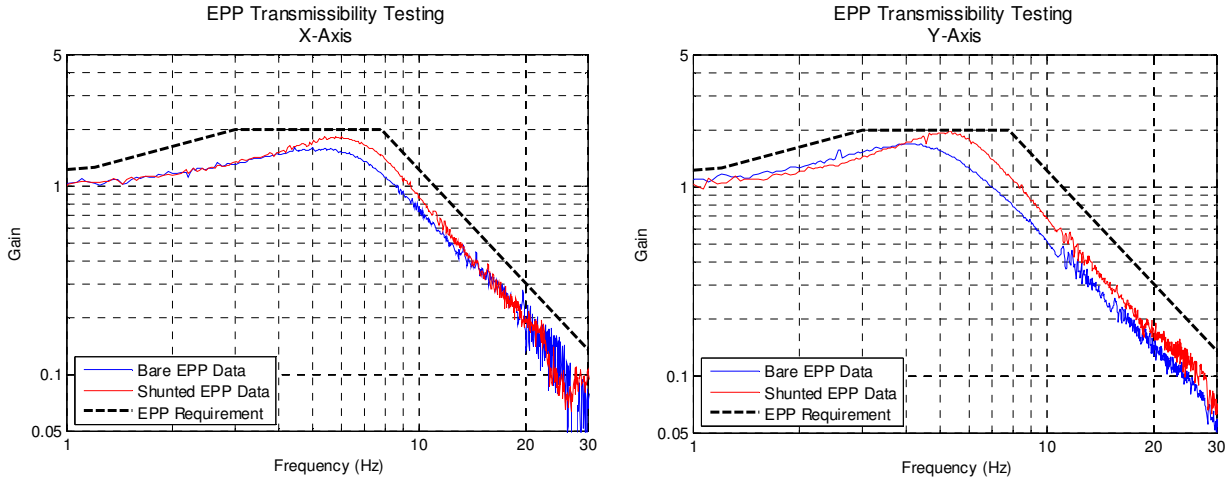

Figure 5. GOES-R EPP Isolation Requirements and Observed EDU Testing Performance.[7]

As Honeywell completed an EDU RWA and Moog CSA completed an EDU isolator, the separate elements were shipped to NASA Goddard for integrated Kistler Table testing. Two configurations were tested. The two configurations were identical with the exception that the RWA was hard mounted for one configuration and mounted on the Moog CSA isolator for the other. The hard mounts were designed to keep the RWA center-of-gravity at exactly the same location relative to the Kistler table as the isolated configuration. The measured Z-axis (RWA spin axis) force disturbances over the nominal operational wheel speed range 0-1300 RPM are shown in Figure 6 for both the hard mounted and isolated configurations. The improvement in performance over the 200-300 Hz band is consistent with that measured by the Moog CSA modal testing.

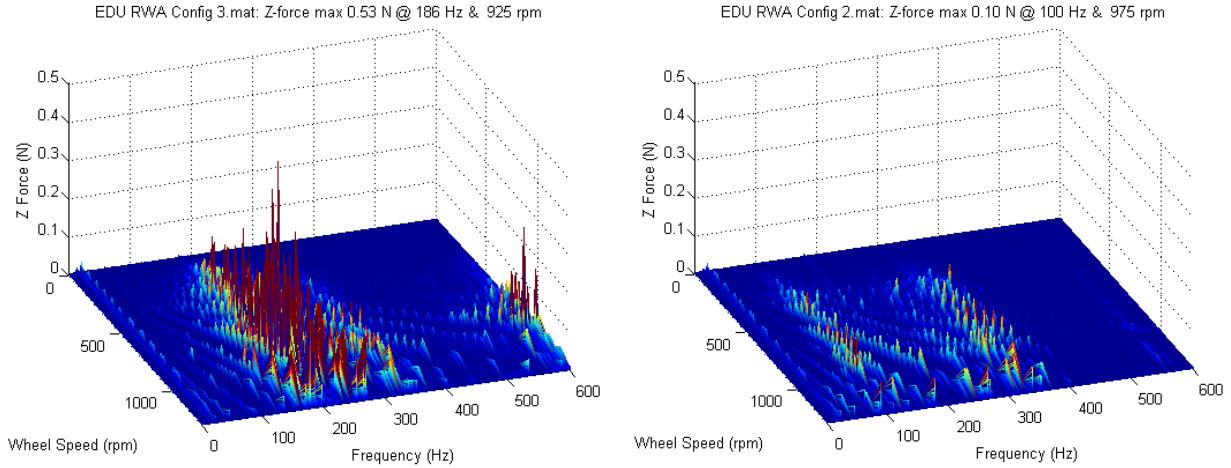

a) Hard Mount Configuration. *b) Isolated Configuration.*

Figure 6. RWA Hard Mount vs Isolated NASA Goddard Kistler Table Induced Vibration Results.

EDA Based in-Flight Results

Following launch, GOES-16 and GOES-17 were subjected to months of extensive testing prior to being put into operational service. Six onboard Engineering Diagnostic Accelerometers (EDAs), seismic accelerometers sampled at ~2 KHz, were used to characterize the disturbance environment at the ABI and GLM interfaces. A stressing scenario includes back-to-back momentum adjust (MA) and stationkeeping (SK) maneuvers, where the RWAs rapidly slew between positive and negative operating speeds. Both low-thrust REA's and arcjets are used during these maneuvers, exciting the vehicle structural modes and the fuel and oxidizer slosh modes. Throughout the maneuvers, all instruments remain fully operational in their nominal states, which includes the ABI scanning and the CC operating.[8]

The SRS response envelopes from the EDA data are shown in Figure 7 for GOES-16 with only the ABI primary CC operating and for GOES-17 with both the ABI primary and redundant CC operating. Despite the CC operating differences, the responses are similar showing large margins relative to the GIRD requirements. The flight results demonstrate that the analysis techniques were conservative, as expected and that the inclusion of both EPP and RWA isolation may not have been absolutely necessary.

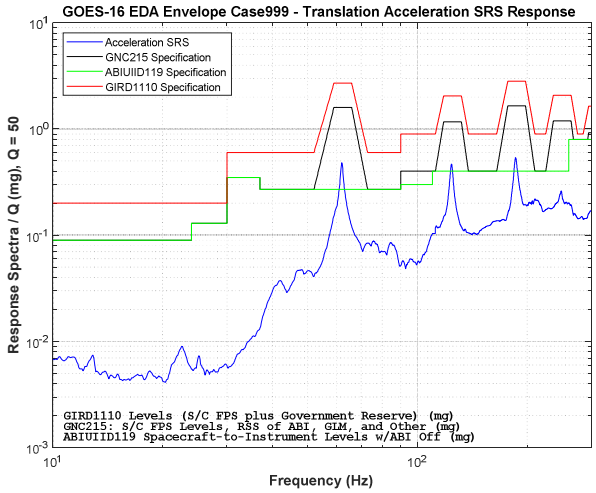

a) GOES-16 w/ ABI Primary CC @ 62.1 Hz and Redundant CC Off.

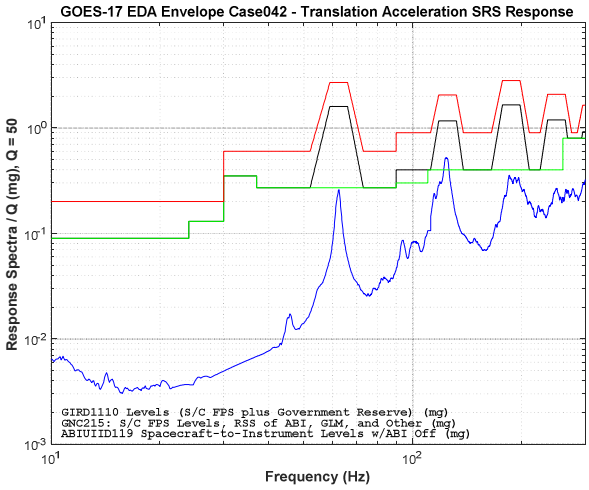

b) GOES-17 w/ ABI Primary CC @ 62.6 Hz and Redundant CC @ 61.6 Hz.

Figure 7. In-Flight EDA Enveloped SRS Response During MA/SK Maneuver.

In response to an unexpected anomaly with the GOES-17 ABI loop heat pipe cooling, in addition to the primary CC, the redundant CC was pressed into service. Although jitter requirements apply only with a single CC operational, the robust design is tolerant to variations in jitter disturbances, enabling simultaneous CC operations. In-flight results show that even with both prime and redundant CCs operating, GIRD requirements are satisfied as shown in Figure 8.

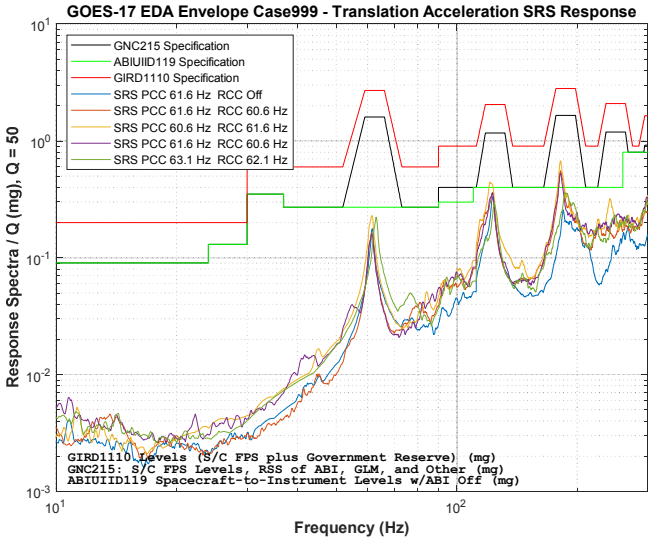

Figure 8. The Simultaneous Operation of Prime and Redundant CCs on GOES-17 was Enabled by the Design Being Robust to Variations in Jitter Disturbances.

IMU Based In-Flight Results

Besides the EPP mounted EDAs, data from the EPP mounted IMU was also processed to assess in-flight jitter performance. The ABI CC harmonics are evident in the IMU measurements. The processed IMU data was sampled at 100 Hz. Figure 9a shows the IMU response to the case where the ABI primary CC was operated at 61.6 Hz with the redundant CC off. The ABI primary CC first two harmonics are at 61.6 Hz and 123.2 Hz. The mechanical motion that results from the CC disturbance at these harmonics are aliased into the IMU 50 Hz Nyquist frequency band to 38.4 Hz and 23.2 Hz, respectively. Both frequencies are visible in the figure. The aliased harmonic frequencies and corresponding amplitudes are such that their impact on INR performance and image quality are insignificant.

Figure 9b shows the IMU response with both CCs on, primary at 63.1 Hz and redundant at 62.1 Hz. The ABI primary CC first two harmonics are at 63.1 Hz and 126.2 Hz which alias into the IMU 50 Hz Nyquist frequency band at 36.9 Hz and 26.2 Hz, respectively. Likewise for the redundant CC operating at 62.1 Hz, the aliased frequencies for the first two harmonics are 37.9 Hz and 24.2 Hz, respectively. All four frequencies are visible in the figure.

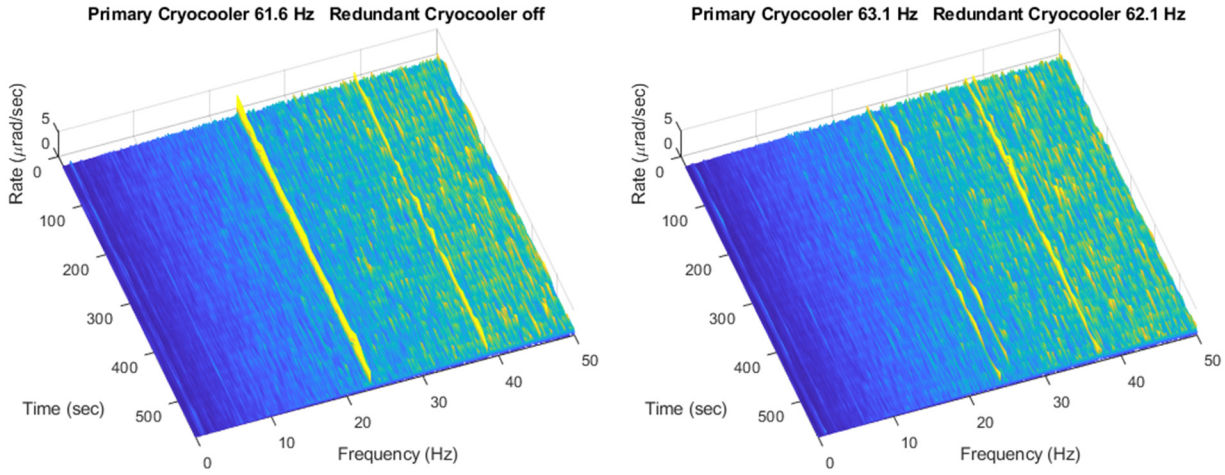

a) Primary CC @ 61.6 Hz and Redundant CC Off.

b) Primary CC @ 63.1 Hz and Redundant CC @ 62.1 Hz.

Figure 9. GOES-17 In-Flight IMU Y-Axis Response Post-EPP Deploy.

ACTIVE VIBRATION DAMPING COMPENSATION

The GOES-R vehicles have several flexible appendages with multiple modal frequencies below 3 Hz, which can result in undesirable pointing perturbations. In order to meet GOES-R pointing and pointing stability requirements, GOES-R implements AVD compensation operating in parallel with the nadir pointing attitude control. Details of the implementation and GOES-16 flight results have been presented previously.[11] AVD compensation provides appropriate modal compensation based upon solar array gimbal angle and sensed body rates. AVD applies phase stabilized compensation at the appendage mode natural frequencies. This increases modal damping and attenuates appendage vibration, thereby improving LOS low frequency pointing performance.

As shown in Figure 10, AVD consists of three components: a FSW algorithm performing in-flight modal excitation, a ground-based system identification process, and a FSW algorithm implementing AVD compensation. The modal excitation consists of 20 Hz pseudo-random reaction wheel torque commands over a single orbit. Time-correlated angular rate data is collected at 20 Hz over this period. Ground processing of flight telemetry produces a Fourier model parameterized by solar array gimbal angle. Additional analysis selects the AVD compensation, providing both acceptable tracking performance and modal attenuation. The identified Fourier model coefficients and the AVD controller gains are then uplinked to the spacecraft. The AVD compensation FSW selects the appropriate coefficients based upon solar array gimbal angle, applies those coefficients to the angular rate data, and outputs reaction wheel torque commands.

In flight characterization is required because AVD is sensitive to small variations in vehicle dynamics. Trying to reuse parameters would not work at all even though the designs are nearly identical. For example, the order of the GOES-16 solution was 140th while the order of the solution for GOES-17 was 180th. The AVD characterization produced a new structural model of GOES-17, significantly different from GOES-16. The identified frequencies and damping ratios for the two vehicles are shown in Table 1.

Figure 10. AVD Implementation Approach.

Table 1. Modal Damping Increase Provided by the GOES-16 & GOES-17 AVD Controllers.

Appendage Flexible Mode Description	SADA Angle (Deg)	Body Axis	S/C	Frequency (Hz)	Damping Ratio (%) Identified	Damping Ratio (%) with AVD	AVD Damping Factor
Solar Wing Out-of-Plane Bending I	0	Roll	G16	0.273	0.253	2.743	10.82
			G17	0.268	0.324	2.913	8.98
Magnetometer Boom X-Rotation Bending	330	Roll	G16	0.691	0.674	0.628	0.93
			G17	0.683	0.917	0.900	0.98
Solar Wing Out-of-Plane Bending II	0	Roll	G16	0.948	0.460	0.878	1.91
			G17	0.908	0.502	1.009	2.01
Antenna Wing Out-of-Plane Bending	All	Pitch	G16	0.999	7.191	7.182	1.00
			G17	0.998	1.100	1.107	1.01
Solar Wing Twist II	All	Pitch	G16	1.320	0.279	0.366	1.31
			G17	1.314	0.280	0.356	1.27
Solar Wing Out-of-Plane Bending III	0	Roll	G16	1.923	0.321	0.305	0.95
			G17	1.892	0.225	0.211	0.94
Antenna Wing In-Plane Bending	0	Yaw	G16	1.996	0.840	1.149	1.37
			G17	2.027	0.826	1.259	1.52

Note: AVD Damping Factor = (Modal Damping with AVD)/(Modal Damping without AVD)

For GOES-17 with a solar array gimbal angle of 0 deg, Figure 11 shows the roll-axis transfer function from disturbance torque input to angular rate output for both AVD compensation enabled and disabled. The modal damping increase provided by AVD can clearly be seen. The AVD compensation increases modal damping significantly for several appendage modes at this gimbal angle, as summarized in Table 1. In particular, AVD provides ~10X increase in the damping of the solar wing out-of-plane fundamental bending mode.

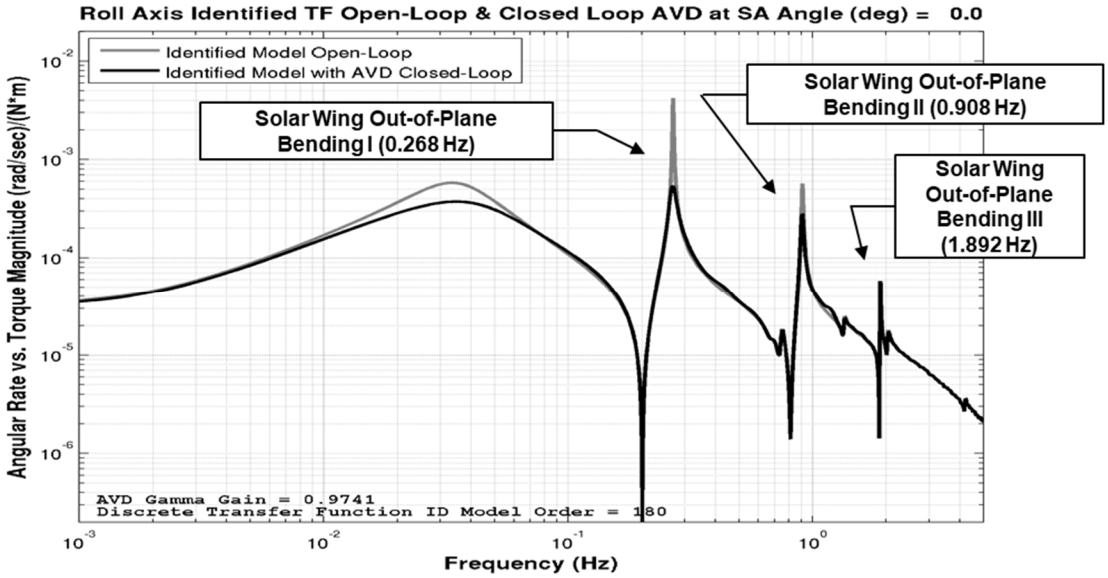

Figure 11. GOES-17 Disturbance Rejection Transfer Function with AVD Disabled and Enabled.

The performance impacts are most evident at the beginning and end of the various thruster operations, namely MA, North-South stationkeeping (NSSK), and East-West stationkeeping (EWSK). An example of the performance improvement with AVD is shown in Figure 12, which shows the attitude error for a pre-AVD NSSK maneuver plotted on the same time scale as a post-AVD enabled NSSK. At the end of NSSK maneuvers, a small attitude transient is typically observed. The thruster torque transient and the control activity to remove the transient can excite the low frequency appendage modes. The end of the NSSK occurs at the 36 min mark in Figure 12, and the transient response can easily be seen. AVD is very effective in damping the 1st solar panel bending mode.

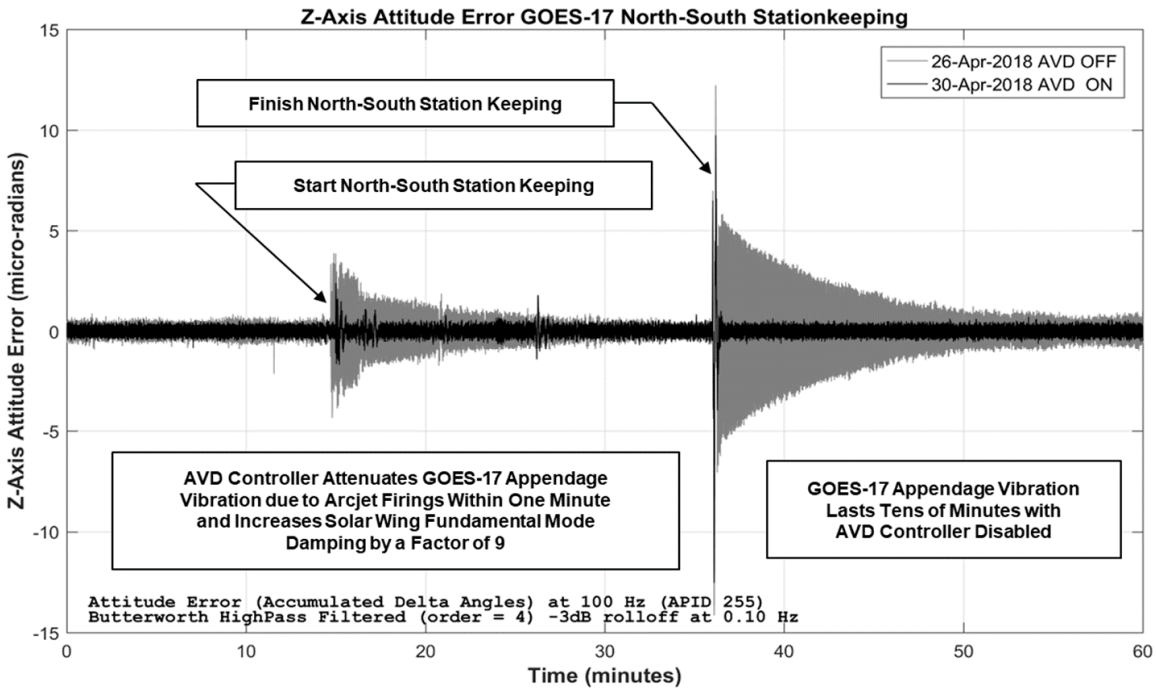

Figure 12. A Dramatic Improvement in LOS Jitter is Clearly Evident with AVD Enabled During a NSSK.

PREDICTED INTERFACE FORCES AND TORQUES COMPENSATION

ABI provides PIFT data packets at 20Hz containing predicted forces and torques, along with predicted timing. The primary disturbance source are the two internal scan mirrors, North-South (NS) and East-West (EW), which provide torques about the instrument X- and Z-axes, respectively. A solar calibration cover is a secondary force, although this is operated less frequently (monthly). These disturbances are compensated for by feeding the torques forward into the attitude controller. Predicted forces are converted to torques using configurable moment arm, and summed with predicted torques. PIFT data are multiplied by configurable gains to correct polarity, and to allow corrections for any performance discrepancies in flight. The FSW issues reaction wheel torques at the time embedded with the PIFT data packet, with additional timing correction for known delays within the system. During the design effort for GOES-R, a 70 millisecond timing error between actual ABI disturbances and a control system response was assumed. This consisted to a 50 ms error (one frame) in system response, and a 20 ms PIFT timing error between PIFT predicted time and the realization of ABI disturbances. The accuracy of the ABI PIFT time tag and the reaction wheel torque command timing was verified prior to launch. However, ground verification of PIFT polarity proved to be extremely difficult, so there were no definitive ground tests to prove the implementation was correct.

Example motion of the ABI instrument's scan mirrors from GOES-17 is shown in the top plot of Figure 13. Unlike AVD which requires unique parameters for each spacecraft, PIFT was unchanged from GOES-16. The motion is typical of normal observations of the continental United States (CONUS). The effectiveness of the PIFT compensation is shown in the bottom two plots of Figure 13, which show the on board rate estimate and rate control error. The PIFT feed forward compensation is enabled at approximately 15:18, as denoted by the red vertical line. Prior to the PIFT compensation being implemented, the rate disturbances from the scan mirrors are approximately 10 µrad/s in the Z-axis. After the compensation is enabled, the response is reduced by an order of magnitude. Significantly smaller responses are also apparent in the X- and Y-axes. This represents exceptional performance considering that the reaction wheels are mounted on the opposite end of the spacecraft from the ABI instrument.

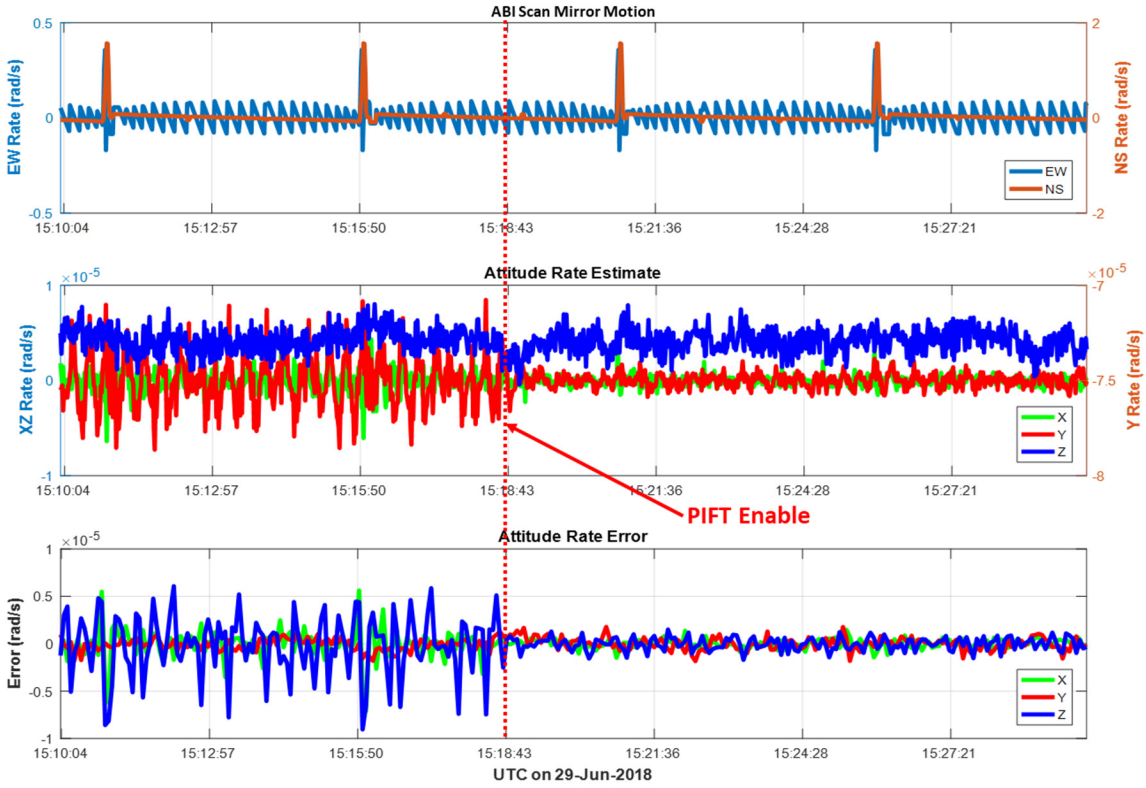

Figure 13. Enabling PIFT Feed-Forward Compensation Greatly Improves LOS Pointing.

INTEGRATED RATE ERROR PERFORMANCE

The spacecraft is required to provide low-latency 3-axis attitude rate data directly to the ABI instrument at 100 Hz, and is also required to provide inertial attitude knowledge to the instruments at 1 Hz. The ABI instrument uses attitude rate data to provide real-time control of its LOS. The instrument maintains its own internal attitude knowledge to achieve the GOES-R INR performance.[5] For the 100 Hz attitude rate data provided to ABI, the GOES-R spacecraft has a unique set of specifications. Rather than specifying the rate errors in terms of traditional Farrenkopf gyro model parameters[18] (angle white noise, angle random walk, and rate random walk) GOES-R defines performance in terms of IRE, which specifies 3-axis integrated rate accuracy over various time intervals. As an attitude knowledge requirement, IRE is distinct from a pointing stability requirement, which represents a limit on the physical motion of the spacecraft over some specific time interval. Instead, IRE represents a knowledge error over a specific time interval, regardless of physical motion.

In the GOES-R attitude determination implementation, the gyro and star tracker measurements are synchronized with the spacecraft control frame to provide the most accurate attitude estimate possible. The IRE requirements specify how much error can be accumulated when integrating SSIRU gyro rates. IRE requirements are specified over different time windows from 1 to 900 seconds. The 1 second window is driven by gyro angle white noise (AWN), whereas the other windows are driven by a combination of AWN, bias stability, Kalman filter bias estimation, and alignment stability. Acceptance testing of the SSIRUs included granite block testing over a 24 hour period, which showed SSIRU's installed on GOES-16 and GOES-17 comply with the IRE requirements.

As was done on GOES-16, GOES-17 100 Hz IMU data was processed to assess the deviation in rate estimates over the various windows. Figure 14 shows 300- and 900-sec IRE windows for a 3-hour quiet period of spacecraft operations, where Instruments were operating in their nominal scanning and data collection modes. The 900-sec window is clearly compliant, but the 300-sec window is right at the requirement limit using this conservative analysis technique. We can conclude that the 300-sec IRE is likely compliant as well because of the conservatism of this analysis. The 1-sec IRE window can be assessed by processing the 100 Hz data and looking at the high frequency PSD behavior. This approach contains disturbances that degrade the AWN estimate. Nevertheless, AWN computed this way is 0.00243 arcsec/rt-Hz, which is compliant with the IRE-derived requirement of 0.00245 arcsec/rt-Hz. The

30-sec IRE windows are more difficult to assess from flight data. The data set needed for this assessment would require the spacecraft to disable attitude control, gimbal control, and instrument operations for some period of time while collecting high rate gyro data and star tracker attitude data. For obvious reasons, the program declined to collect this data set. It is reasonable to conclude that the pre-launch data collection discussed in [1,2] sufficiently verifies the 30-sec IRE requirements. Even though it is difficult to say unequivocally the flight data demonstrate IRE requirement compliance, the flight results are consistent with the pre-launch test data and analysis. The GOES-17 results were in family with GOES-16.

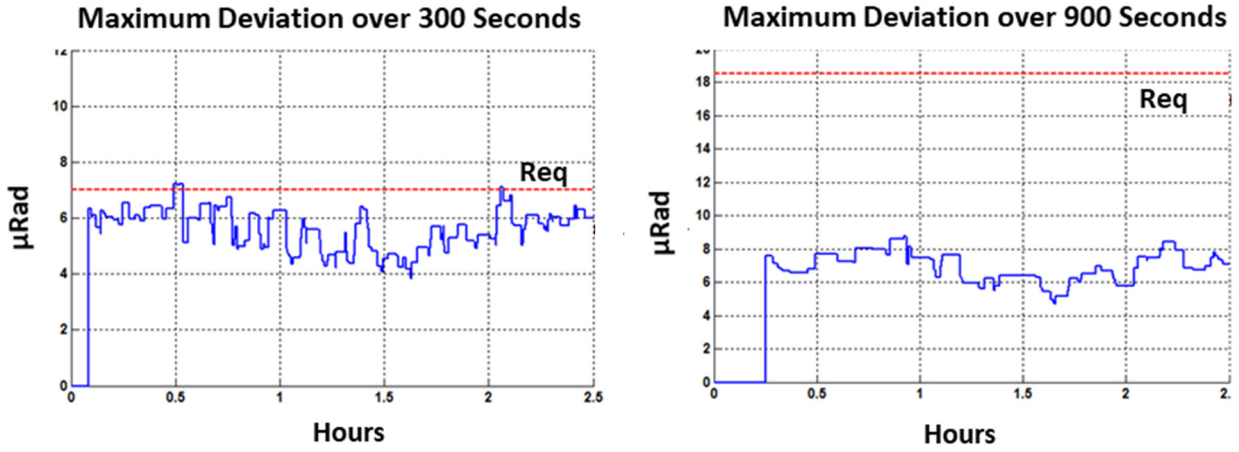

Figure 14. 300 and 900 Second IRE Estimates from GOES-17 Flight Telemetry.

CONCLUSION

The on-orbit commissioning of the GOES-16 and GOES-17 spacecraft has ushered in the next generation of earth, solar and space weather observations with quantum improvements in spectral, spatial and temporal resolution. The realization of this performance imposed demanding pointing stability and jitter requirements on the GN&C subsystem, which were achieved through the use of several key enabling technologies. Passive isolation of both the optical bench and the reaction wheels successfully attenuated jitter at higher frequencies, while AVD provides increased damping for lower frequency structural modes, allowing the GOES-R series spacecraft to operate through MA and SK maneuvers. PIFT, the 2-way data interface between the spacecraft GN&C subsystem and the instrument provided for attenuation of instrument-induced disturbances and provided the capability for the instrument LOS controller to steer out jitter up to the first instrument mode. As we have shown in this paper, the in-flight performance of the GN&C design provides the necessary capabilities to achieve the demanding GOES-R mission objectives. Its robust design enabled the simultaneous operation of the ABI prime and redundant CCs to resolve an in-flight cooling anomaly on GOES-17; above and beyond original expectations.

ACKNOWLEDGMENTS

This work was performed at Lockheed Martin Space Systems, under NASA contract NNG09HR00C, and at the National Aeronautics and Space Administration Goddard Space Flight Center. The authors gratefully acknowledge the many individuals who contributed in various ways through GOES-R program workshops and reviews, and helped developed a better understanding between instrument operations and spacecraft performance. The authors extend a special acknowledgement to Brian Clapp for his contributions to the GOES GN&C design, particularly in jitter modeling and compensation area. The resulting implementation provides a quantum increase in Earth and Solar weather monitoring capabilities.

REFERENCES

[1] J. Chapel, D. Stancliffe, T. Bevacqua, S. Winkler, B. Clapp, T. Rood, D. Gaylor, D. Freesland, A. Krimchansky, "Guidance, Navigation, and Control Performance for the GOES-R Spacecraft," Proceedings of the 9th International ESA Conference on Guidance, Navigation & Control Systems, Oporto, Portugal, Jun 2014.

[2] J. Chapel, D. Stancliffe, T. Bevacqua, S. Winkler, B. Clapp, T. Rood, D. Gaylor, D. Freesland, A. Krimchansky, "Guidance, Navigation, and Control Performance for the GOES-R Spacecraft," CEAS Space Journal, DOI 10.1007/s12567-015-0077-1, March 2015.

[3] J. Chapel, D. Stancliffe, T. Bevacqua, S. Winkler, B. Clapp, T. Rood, D. Freesland, A. Reth, D. Early, T. Walsh, A. Krimchansky, "In-Flight Guidance, Navigation, and Control Performance Results for the GOES-16 Spacecraft," Proceedings of the 10th International ESA Conference on Guidance, Navigation & Control Systems, Salzburg, Austria, May 2017.

[4] T. J. Schmit, Jun Li, Jinlong Li, W. F. Feltz, J. J. Gurka, M. D. Goldberg, K. J. Schrab, "The GOES-R Advanced Base-line Imager and the Continuation of Current Sounder Products," J. Appl. Meteor. Climatol., 47, 2696–2711.

[5] D. Igli, 2013, "GOES-R Advanced Baseline Imager Precise Pointing Control and Image Collection," Proceedings of the 2013 AAS Guidance and Control Conference, Breckenridge, CO, Feb 2013.

[6] L. P. Davis, D. R. Carter, T. T. Hyde, "Second-Generation Hybrid D-Strut," Proc. SPIE 2445, Smart Structures and Materials 1995: Passive Damping, 161, May 1995.

[7] D. Freesland, D. Carter, J. Chapel, B. Clapp, J. Howat, and A. Krimchansky, "GOES-R Dual Isolation," Proceedings of the 2015 AAS Guidance and Control Conference, Breckenridge, CO, Feb 2015.

[8] D. Carter, B. Clapp, D. Early, D. Freesland, J. Chapel, R. Bailey, A. Krimchansky, "GOES-16 On-Orbit Dual Isolation Performance Characterization Results," Proceedings of the 10th International ESA Conference on Guidance, Navigation & Control Systems, Salzburg, Austria, Jun 2017.

[9] C. D. Johnson, J. M. Howat, P. S. Wilke, "Vibration Isolation System and Method," U.S. Patent 20140084527A1, Moog, Inc., Publication Date Mar 27, 2014.

[10] D. Freesland, A. Reth, A. Krimchansky, M. Donnelly, Tim Walsh, "Improving Attitude Stability Performance on GOES-R Using PIFT," Proceedings of the 2007 AAS Guidance and Control Conference, Breckenridge, CO, Feb 2007.

[11] B. R. Clapp, H. J. Weigl, N. E. Goodzeit, D. R. Carter, and T. J. Rood, "GOES-R Active Vibration Damping Controller Design, Implementation, and On-Orbit Performance," Proceedings of the 10th International ESA Conference on Guidance, Navigation & Control Systems, Salzburg, Austria, Jun 2017.

[12] N. E. Goodzeit, H. J. Weigl, "Active Vibration Damping (AVD) System for Precision Pointing Spacecraft," U.S. Patent WO2008136881A1, Lockheed Martin, Publication Date Nov 13, 2008.

[13] E. J. Lefferts, F. L. Markley, and M. D. Shuster, "Kalman Filtering for Spacecraft Attitude Estimation," Journal of Guidance, Sep-Oct, 1982, Vol 5, No 5, p. 417.

[14] D. Igli, V. Virgilio and K Grounder, 2009, "Image Navigation and Registration for GOES-R Advanced Baseline Imager," Proceedings of the 2009 AAS G&C Conference, Breckenridge, CO, Feb 2009.

[15] J. Chapel, E. Schmitz, W. Sidney, M. Johnson, P. Good, J. Wynn, T. Bayer, "Attitude Control Performance for MRO Aerobraking and the Initial Science Phase," Proceedings of the 2007 AAS Guidance and Control Conference, Brecken-ridge, CO, Feb 2007.

[16] GOES-R General Interface Requirements Document (GIRD), 417-R-GIRD-0009, Version 2.33, July 29, 2013.

[17] GOES-R Series Payload Resource Allocation Document (PRAD), 417-R-RAD-0061, Version 2.21, June 14, 2013.

[18] R. L. Farrenkopf, "Analytic Steady-State Accuracy Solutions for Two Common Spacecraft Attitude Estimators," Journal of Guidance, Control, and Dynamics, Vol. 1, No. 4 (1978), pp. 282-284.